Multimedia Contents

4. Mechanism and Actuation

Victor Scheinman, J. Michael McCarthy, Jae-Bok Song

This chapter focuses on the principles that guide the design and construction of robotic systems. The kinematics equations and Jacobian of the robot characterize its range of motion and mechanical advantage, and guide the selection of its size and joint arrangement. The tasks a robot is to perform and the associated precision of its movement determine detailed features such as mechanical structure, transmission, and actuator selection. Here we discuss in detail both the mathematical tools and practical considerations that guide the design of mechanisms and actuation for a robot system.

The following sections (Sect. 4.1) discuss characteristics of the mechanisms and actuation that affect the performance of a robot. Sections 4.2–4.6 discuss the basic features of a robot manipulator and their relationship to the mathematical model that is used to characterize its performance. Sections 4.7 and 4.8 focus on the details of the structure and actuation of the robot and how they combine to yield various types of robots. The final Sect. 4.9 relates these design features to various performance metrics.

4.1 Overview

The physical structure such as the beams, links, castings, shafts, slides, and bearings of a robot that create its movable skeleton is termed the mechanical structure or mechanism of the robot. The electric, hydraulic and pneumatic motors and other elements that cause the links of the mechanism to move are called actuators. In this chapter we consider the variety of designs for the mechanisms and actuators that result in a machine system that transforms computer commands into versatile physical movement.

Early robots were designed with general motion capability under the assumption that they would find the largest market if they could perform the widest variety of tasks; this emphasis on flexibility proved to be expensive in both cost and performance. Robots are now often designed for specific applications and to perform limited sets of tasks.

Robot design focuses on the number of joints, physical size, payload capacity, and the movement requirements of the end-effector. The configuration of the movable skeleton and the overall size of the robot are determined by task requirements for reach, workspace, and reorientation ability. These features affect the precision of end-effector path control needed for applications such as for arc-welding and for the smooth movement of paint spraying. They also define the absolute positioning capability necessary for small part assembly, the repeatability needed for material and package handling, and the fine resolution that allows precise, real-time sensor-based motions.

A critical concern in robotic system design is the range of tasks the robot is expected to perform. The robot should be designed to have the flexibility it needs to perform the range of tasks for which it is intended. This determines the topology of the robot mechanism and the actuator system. The choices of geometry, material, sensors, and cable routing follow from these basic decisions.

4.2 System Features

The primary features that characterize a robot are its work envelope and load capacity.

4.2.1 Work Envelope

The space in which a robot can operate is its work envelope, which encloses its workspace. While the workspace of the robot defines positions and orientations that it can achieve to accomplish a task, the work envelope also includes the volume of space the robot itself occupies as it moves. This envelope is defined by the types of joints, their range of movement and the lengths of the links that connect them. The physical size of this envelope and the loads on the robot within this envelope are of primary consideration in the design of the mechanical structure of a robot.

Robot work envelope layouts must include considerations of regions of limited accessibility where the mechanical structure may experience movement limitations. These constraints arise from limited joint travel range, link lengths, the angles between axes, or a combination of these. Revolute joint manipulators generally work better in the middle of their work envelopes than at extremes (Fig. 4.1). Manipulator link lengths and joint travel should be chosen to leave margins for variable sensor-guided controlled path motions and for tool or end-effector changes, as offsets and length differences will often alter the work envelope.

4.2.2 Load Capacity

Load capacity, a primary robot specification, is closely coupled with acceleration and speed. For assembly robots, mechanism acceleration and stiffness (structure and drive stiffness) are often more important design parameters than peak velocity or maximum load capacity, as minimizing pick-and-place motion cycle time, while maintaining placement precision, is generally a top priority in small part assembly. In the case of arc-welding, where slow controlled-path motion is required, velocity

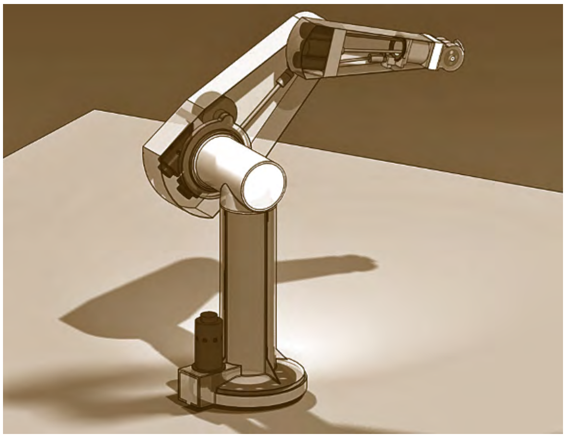

Fig. 4.1 The PUMA 560 robot

jitter and weld path-following accuracy are important. Load capacity should be seen as a variable. It is wise to design and specify a manipulator in terms of useful payload as a function of performance rather than just in terms of maximum capacity.

Load capacity specifications must take into account gravity and inertial loading seen at the end-effector. These factors strongly affect wrist, end-effector design and drive selection. In general, load capacity is more a function of manipulator acceleration and wrist torque than any other factor. The load rating also affects manipulator static structural deflection, steady-state motor torque, system natural frequency, damping, and the choice of control system parameters for best performance and stability.

4.2.3 Kinematic Skeleton

Manipulator shape and size is determined by requirements on its workspace shape and layout, the precision of its movement, its acceleration and speed, and its construction. Cartesian manipulators have the simplest transform and control equation solutions. Their prismatic (straight-line motion) and orthogonal (perpendicular) axes make motion planning and computation relatively straightforward. Because their major motion axes do not couple dynamically (to a first order), their control equations are also simplified. Manipulators with all revolute (rotary) joints are generally harder to control, but they feature a more compact and efficient structure for a given working volume. It is generally easier to design and build a good revolute joint than a long motion prismatic joint. The workspaces of revolute joint manipulators can easily overlap for coordinated multi-robot installations, in contrast to the more exclusive useful workspace of gantry style robots.

Final selection of the robot configuration should capitalize on specific kinematic, structural or performance requirements. For example, a requirement for a very precise vertical straight-line motion may dictate the choice of a simple prismatic vertical axis rather than two or three revolute joints requiring coordinated control.

Six degrees of freedom (DOFs) are the minimum required to place the end-effector or tool of a robotic manipulator at any arbitrary location (position and orientation) within its accessible workspace. Most simple or preplanned tasks can be performed with fewer than six DOFs by careful task setup to eliminate certain axis motions, or because the tool or task does not require full specification of location. An example of this is vertical assembly using a powered screwdriver, where all operations can be achieved with three degrees of freedom.

Some applications require the use of manipulators with more than six DOFs, in particular when mobility or obstacle avoidance are necessary. For example, a pipe-crawling maintenance robot requires control of the robot shape as well as precise positioning of its end-effector. Generally, adding degrees of freedom increases cycle time and reduces load capacity and accuracy for a given manipulator configuration and drive system.

4.3 Kinematics and Kinetics

The dynamics of a robot can be separated into the properties of the movement that depend upon the geometry of its mechanical structure, termed *kinematics*, and those that depend on forces that act on the system, known as *kinetics*. It is a law of dynamics that the difference between the change in energy of the moving robot and the work performed by the forces acting on it does not change over small variations of its trajectory. This is called the *principle of virtual work* and states that variations in work and energy must cancel for all virtual displacements [4.1, 2].

Because machines such as robots are designed to minimize energy losses, often due to joint friction and material strain losses, we can assume that the variation in energy is small. This means that the work input of the actuators is nearly equal to the work of the output forces.

If we consider this relationship over a small duration of time, we have that the time rate of input work, or input power is nearly equal to the associated output power. Because power is force times velocity, we obtain the fundamental relationship that the ratio of input to output forces is the reciprocal of the ratio of input to output speeds. Another way of saying this is that, in the ideal machine, *the mechanical advantage of a machine is the inverse of its speed ratio.*

4.3.1 Robot Topology

The kinematic skeleton of a robot is modeled as a series of links connected by either hinged or sliding joints forming a serial chain. This skeleton has two basic forms, that of a single serial chain called a *serial robot* (Fig. 4.1) and as a set of serial chains supporting a single end-effector, called a *parallel robot*, such as the platform shown in Fig. 4.2. Robots can be configured to work in parallel such as the individual legs of walking machines (Figs. 4.3 and 4.4) [4.3], as

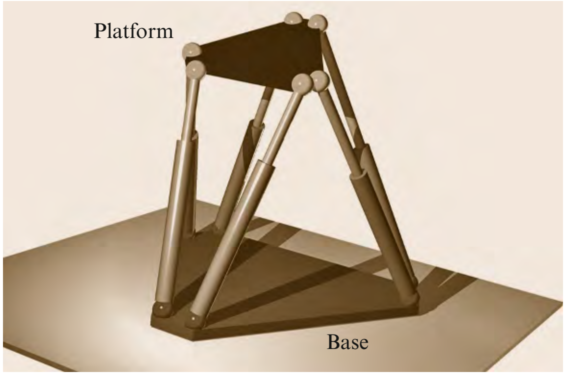

Fig. 4.2 A parallel robot can have as many as six serial chains that connect a platform to the base frame (VIDEO 640)

Fig. 4.3 A photograph of the adaptive suspension vehicle (ASV)walking machine

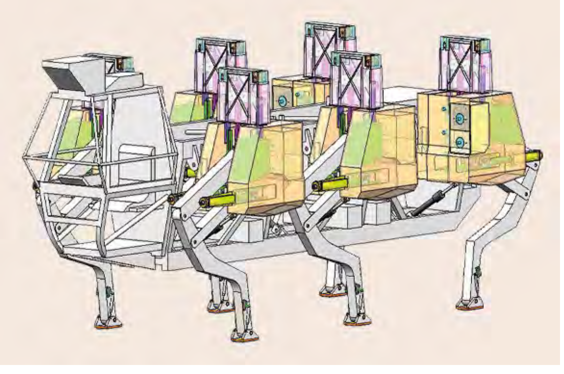

Fig. 4.4 The adaptive suspension vehicle walking machine

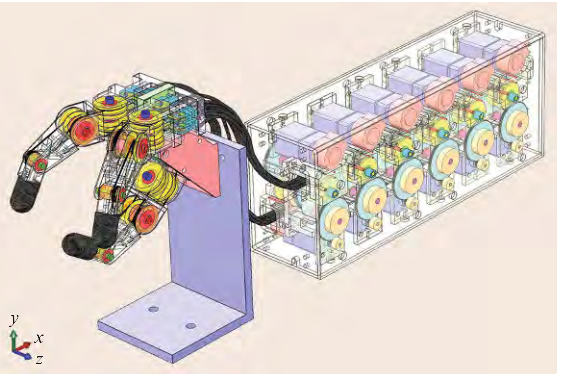

Fig. 4.5 The Salisbury three-fingered robot hand with its cable drive system

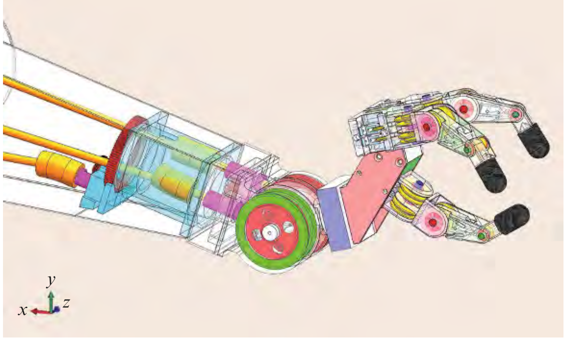

Fig. 4.6 The Salisbury hand as the end-effector of a PUMA robot (the drive system is not shown)

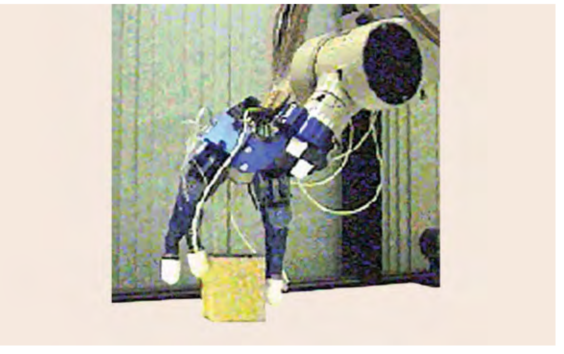

Fig. 4.7 A photograph of the Salisbury three-fingered hand grasping a block

well as the fingers of mechanical hands (Figs. 4.5–4.7 and VIDEO 642) [4.4].

The robot end-effector is the preferred tool for interaction with the environment, and the ability to position and orient this end-effector is defined by the skeleton of the robot. In a general serial robot, a chain of six joints provides full control over the end-effector. In a general parallel robot, there are more than six joints and the six actuators may be applied to these joints in a variety of ways to control the movement of the end-effector.

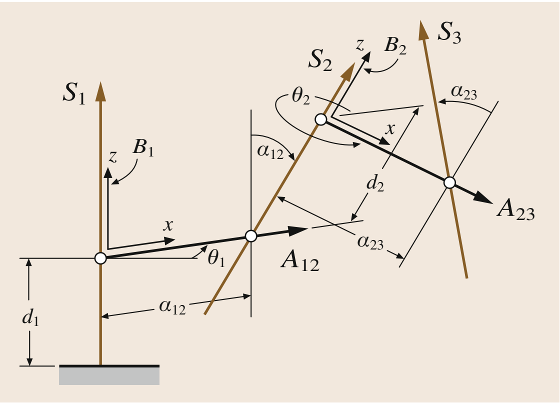

Fig. 4.8 The kinematic skeleton defined by the join axes and their common normals

4.3.2 Kinematics Equations

A robot is designed so that specifying the values of local joint parameters, such as the angle of rotary joints and the travel of sliding joints, specifies the position of every component of a machine using its kinematics equations. To do this the robot is described by a sequence of lines representing the axes $\hat{z}_j$ of equivalent revolute or prismatic joints and the common normal lines $\hat{x}_j$ which form the kinematic skeleton of the chain (Fig. 4.8). This construction allows the specification of the location of each link of the robot relative to the base by the matrix equation

$$\mathbf{T} = \mathbf{Z}(\theta_1, d_1)\mathbf{X}(\alpha_1, a_1)\mathbf{Z}(\theta_2, d_2)\ldots \times \mathbf{X}(\alpha_{m-1}, a_{m-1})\mathbf{Z}(\theta_m, d_m)\,, \quad (4.1)$$

known as the *kinematics equations* of the chain [4.5, 6] (Chap. 2; (2.46)). The set of all positions $\mathbf{T}$ that the end-effector can reach for all values of the joint parameters is called the *workspace* of the robot.

The matrices $\mathbf{Z}(\theta_j, d_j)$ and $\mathbf{X}(\alpha_j, a_j)$ are 4×4 matrices that define screw displacements around and along the joint axes $\hat{z}_j$ and $\hat{x}_j$, respectively [4.7]. The parameters α_j and a_j define the dimensions of the links in the chain. The parameter θ_j is the joint variable for revolute joints and d_j is the variable for prismatic joints. The trajectory ${}^F\boldsymbol{p}(t)$ of a point ${}^M\boldsymbol{p}$ in the end-effector is obtained from the joint trajectory,

$$\boldsymbol{q}(t) = (q_1(t), \ldots, q_m(t))^{\mathrm{T}}\,,$$

where q_i is either θ_i or d_i depending on the joint, given by

$${}^F\boldsymbol{p}(t) = \mathbf{T}(\boldsymbol{q}(t))^M\boldsymbol{p}\,. \quad (4.2)$$

If the end-effector is connected to the base frame by more than one serial chain (Fig. 4.2) then we have a set of kinematics equations for each chain,

$$\mathbf{T} = \mathbf{B}_j\mathbf{T}(\boldsymbol{q}_j)\mathbf{E}_j, \quad j = 1, \ldots, n\,, \quad (4.3)$$

where $\mathbf{B}_j$ locates the base of the j-th chain and $\mathbf{E}_j$ defines the position of its attachment to the part, or end-effector. The set of positions $\mathbf{T}$ that simultaneously satisfy all of these equations is the workspace of the part. This imposes constraints on the joint variables that must be determined to define its workspace completely [4.8, 9].

4.3.3 Configuration Space

The kinematics equations of the robot relate the range of values available for the joint parameters, called the configuration space of the robot, to the workspace of the end-effector. This configuration space is a fundamental tool in robot path planning for obstacle avoidance [4.10]. Though any link in the chain forming a robot may hit an obstacle, it is the end-effector that is intended to approach and move around obstacles such as the table supporting the robot and the fixtures for parts it is to pick up. Obstacles define forbidden positions and orientations in the workspace which map back to forbidden joint angles in the configuration space of the robot. Robot path planners seek trajectories to a goal position through the free space around these joint space obstacles [4.11].

4.3.4 Speed Ratios

The speed ratios of a robot relate the velocity ${}^F\dot{\boldsymbol{p}}$ of a point ${}^F\boldsymbol{p}$ in the end-effector to the joint rates

$$\dot{\boldsymbol{q}} = (\dot{q}_1, \ldots, \dot{q}_m)^{\mathrm{T}}\,,$$

that is

$${}^F\dot{\boldsymbol{p}} = \boldsymbol{v} + \boldsymbol{\omega} \times \left({}^F\boldsymbol{p} - \boldsymbol{d}\right)\,, \quad (4.4)$$

where $\boldsymbol{d}$ and $\boldsymbol{v}$ are the position and velocity of a reference point, respectively, and $\boldsymbol{\omega}$ is the angular velocity of the end-effector.

The vectors $\boldsymbol{v}$ and $\boldsymbol{\omega}$ depend on the joint rates $\dot{q}_j$ through the formula

$$\begin{pmatrix}\boldsymbol{v}\\ \boldsymbol{\omega}\end{pmatrix} = \begin{pmatrix}\frac{\partial \boldsymbol{v}}{\partial \dot{q}_1} & \frac{\partial \boldsymbol{v}}{\partial \dot{q}_2} & \cdots & \frac{\partial \boldsymbol{v}}{\partial \dot{q}_m}\\ \frac{\partial \boldsymbol{\omega}}{\partial \dot{q}_1} & \frac{\partial \boldsymbol{\omega}}{\partial \dot{q}_2} & \cdots & \frac{\partial \boldsymbol{\omega}}{\partial \dot{q}_m}\end{pmatrix}\begin{pmatrix}\dot{q}_1\\ \vdots\\ \dot{q}_m\end{pmatrix}, \quad (4.5)$$

or

$$\mathbf{v} = \mathbf{J}\dot{\boldsymbol{q}} \,. \tag{4.6}$$

The coefficient matrix **J** in this equation is called the *Jacobian* and is a matrix of speed ratios relating the velocity of the tool to the input joint rotation rates [4.6, 9].

4.3.5 Mechanical Advantage

If the end-effector of the robot exerts a force $\boldsymbol{f}$ at the point ${}^F\boldsymbol{p}$, then the power output is

$$P_{\text{out}} = \boldsymbol{f} \cdot {}^F\dot{\boldsymbol{p}} = \sum_{j=1}^{m} \boldsymbol{f} \cdot \left[\frac{\partial \boldsymbol{v}}{\partial \dot{q}_j} + \frac{\partial \boldsymbol{\omega}}{\partial \dot{q}_j} \times \left({}^F\boldsymbol{p} - \boldsymbol{d}\right) \right] \dot{q}_j \,. \tag{4.7}$$

Each term in this sum is the portion of the output power that can be associated with an actuator at joint S_j, if one exists.

The power input at joint S_j is the product $\tau_j \dot{q}_j$ of the torque τ_j and joint angular velocity $\dot{q}_j$. Using the principle of virtual work for each joint we can compute

$$\tau_j = \boldsymbol{f} \cdot \frac{\partial \boldsymbol{v}}{\partial \dot{q}_j} + \left({}^F\boldsymbol{p} - \boldsymbol{d}\right) \times \boldsymbol{f} \cdot \frac{\partial \boldsymbol{\omega}}{\partial \dot{q}_j}, \quad j = 1, \ldots, m \,. \tag{4.8}$$

We have arranged this equation to introduce the force-torque vector

$$\mathsf{f} = (\boldsymbol{f}, ({}^F\boldsymbol{p} - \boldsymbol{d}) \times \boldsymbol{f})^{\mathrm{T}}$$

at the reference point $\boldsymbol{d}$.

The equations (4.8) can be assembled into the matrix equation

$$\boldsymbol{\tau} = \mathbf{J}^{\mathrm{T}} \mathsf{f} \,, \tag{4.9}$$

where **J** is the *Jacobian* defined above in (4.5). For a chain with six joints this equation can be solved for the output force-torque vector f,

$$\mathsf{f} = \left(\mathbf{J}^{\mathrm{T}}\right)^{-1} \boldsymbol{\tau} \,. \tag{4.10}$$

Thus, the matrix that defines the mechanical advantage for this system is the inverse of the matrix of speed ratios.

4.4 Serial Robots

A serial chain robot is a sequence of links and joints that begins at a base and ends with an end-effector (Fig. 4.9). The links and joints of a robot are often configured to provide separate translation and orientation structures. Usually, the first three joints are used to position a reference point in space and the last three form the *wrist* which orients the end-effector around this point [4.12, 13]. This reference point is called the *wrist center*. The volume of space in which the wrist center can be placed is called the *reachable workspace* of the robot. The rotations available at each of these points is called the *dexterous workspace*.

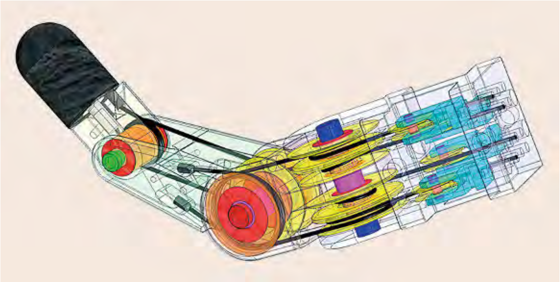

Fig. 4.9 A single finger of the Salisbury hand is a serial chain robot

The design of a robot is often based on the symmetry of its reachable workspace. From this point of view there are three basic shapes: rectangular, cylindrical, and spherical [4.6].A rectangular workspace is provided by three mutually perpendicular prismatic (P) joints which form a PPPS chain called a *Cartesian* robot – S denotes a spherical wrist which allows all rotations about its center point. A rotary base joint combined with two prismatic joints forms a CPS chain with a cylindrical workspace – C denotes a rotary (R) and sliding (P) joint with the same axis. The P-joint can be replaced by a revolute (R) joint that acts as an elbow in order to provide the same radial movement. Finally, two rotary joints at right angles form a T-joint at the base of the robot that supports rotations about a vertical and horizontal axes. Radial movement is provided either by a P-joint, or by an R-joint configured as an elbow. The result is a TPS or TRS chain with a spherical workspace.

It is rare that the workspace is completely symmetrical because joint axes are often offset to avoid link collisions and there are limits to joint travel which combine to distort the shape of the workspace.

4.4.1 Design Optimization

Another approach to robot design uses a direct specification of the workspace as a set of positions for the end-effector of a robotic system [4.14–17] which we call the *task space*. A general serial robot arm has two design parameters, link offset and twist, for each of five links combined with four parameters each that locate the base of the robot and the workpiece in its end-effector, making a total of 18 design variables. The link parameters are often specified so the chain has a spherical wrist and specific workspace shape. The design goal is usually to determine the workspace volume and locate the base and workpiece frames so that the workspace encloses the specified task space.

The task space is defined by a set of 4×4 transformations $\mathbf{D}_i, i = 1, \ldots, k$. The problem is solved iteratively by selecting a design and using the associated kinematics equations $\mathbf{T}(\boldsymbol{q})$ to evaluate relative displacements in the objective function

$$f(\boldsymbol{r}) = \sum_{i=1}^{k} \left\| \mathbf{D}_i \mathbf{T}^{-1}(\boldsymbol{q}_i) \right\| . \quad (4.11)$$

Optimization techniques yield the design parameter vector $\boldsymbol{r}$ that minimizes this objective function.

This optimization depends on the definition of the distance measure between the positions reached by the end-effector and the desired workspace. *Park* [4.18], *Martinez* and *Duffy* [4.19], *Zefran* et al. [4.20], *Lin* and *Burdick* [4.21], and others have shown that there is no distance metric that is coordinate frame invariant. This means that, unless this objective function can be forced to zero so the workspace completely contains the task space, the resulting design will not be *geometric* in the sense that the design is not independent of the choice of coordinates.

4.4.2 Speed Ratios

A six-axis robot has a 6×6 Jacobian $\mathbf{J}$ obtained from (4.5) that is an array of speed ratios relating the components of the velocity $\boldsymbol{v}$ of the wrist center and the angular velocity $\boldsymbol{\omega}$ of the end-effector to each of the joint velocities. Equation (4.9) shows that this Jacobian defines the force-torque vector $\boldsymbol{f}$ exerted at the wrist center in terms of the torque applied by each of the actuators. The link parameters of the robot can be selected to provide a Jacobian $\mathbf{J}$ with specific properties.

The sum of the squares of the actuator torques of a robot is often used as a measure of *effort* [4.22, 23]. From (4.9) we have

$$\boldsymbol{\tau}^{\mathrm{T}} \boldsymbol{\tau} = \boldsymbol{f}^{\mathrm{T}} \mathbf{J} \mathbf{J}^{\mathrm{T}} \boldsymbol{f} . \quad (4.12)$$

The matrix $\mathbf{J}\mathbf{J}^{\mathrm{T}}$ is square and positive definite. Therefore, it can be viewed as defining a hyperellipsoid in six-dimensional space [4.24]. The lengths of the semi-diameters of this ellipsoid are the inverse of the absolute value of the eigenvalues of the Jacobian $\mathbf{J}$. These eigenvalues may be viewed as *modal* speed ratios that define the amplification associated with each joint velocity. Their reciprocals are the associated *modal* mechanical advantages, so the shape of this ellipsoid illustrates the force amplification properties of the robot.

The ratio of the largest of these eigenvalues to the smallest, called the condition number, gives a measure of the anisotropy or *out-of-roundness* of the ellipsoid. A sphere has a condition number of one and is termed *isotropic*. When the end-effector of a robot is in a position with an isotropic Jacobian there is no amplification of the speed ratios or mechanical advantage. This is considered to provide high-fidelity coupling between the input and output because errors are not amplified [4.25, 26]. Thus, the condition number is used as a criterion in a robot design [4.27].

In this case, it is assumed that the basic design of the robot provides a workspace that includes the task space. Parameter optimization finds the internal link parameters that yield the desired properties for the Jacobian. As in minimizing the distance to a desired workspace, optimization based on the Jacobian depends on a careful formulation to avoid coordinate dependency.

4.5 Parallel Robots

A robotic system in which two or more serial chain robots support an end-effector is called a *parallel robot*. For example, the adaptive suspension vehicle (ASV) leg (Fig. 4.10), is a pantograph mechanism driven by parallel actuation. Each supporting chain of a parallel robot may have as manyas six degrees of freedom, however, in general only a total of six joints in the entire system are actuated. A good example is the Stewart platform formed from six TPS robots in which usually only the prismatic joint (P-joint) in each chain is actuated (Fig. 4.2) [4.9, 28, 29].

The kinematics equations of the TPS legs are

$$\mathbf{T} = \mathbf{B}_j \mathbf{T}(\boldsymbol{\theta}_j) \mathbf{E}_j, \quad j = 1, \ldots, 6 , \quad (4.13)$$

where $\mathbf{B}_j$ locates the base of the leg and $\mathbf{E}_j$ defines the position of its attachment to the end-effector. The set of positions $\mathbf{T}$ that simultaneously satisfy all of these equations is the workspace of the parallel robot.

Often the workspace of an individual chain of a parallel robot can be defined by geometric constraints, for example, a position $\mathbf{T}$ is in the workspace of the j-th supporting TPS chain if it satisfies the constraint equation

$$(\mathbf{T}\boldsymbol{x}_j - \boldsymbol{p}_j)\cdot(\mathbf{T}\boldsymbol{x}_j - \boldsymbol{p}_j) = \rho_j^2 \;. \tag{4.14}$$

This equation defines the distance between the base joint $\boldsymbol{p}_j$ and the point of attachment ${}^F\boldsymbol{x}_j = \mathbf{T}\boldsymbol{x}_j$ to the platform as the length ρ_j is controlled by the actuated prismatic joint. In this case the workspace is the set of positions $\mathbf{T}$ that satisfy all six equations, one for each leg.

4.5.1 Workspace

The workspace of a parallel robot is the intersection of the workspaces of the individual supporting chains. However, it is not the intersection of the reachable and dexterous workspaces separately. These workspaces are intimately combined in parallel robots. The dexterous workspace is usually largest near the center of the reachable workspace and shrinks as the reference point moves toward the edge. A focus on the symmetry of movement allowed by supporting leg designs has been an important design tool resulting in many novel parallel designs [4.30, 31]. Simulation of the system is used to evaluate its workspace in terms of design parameters.

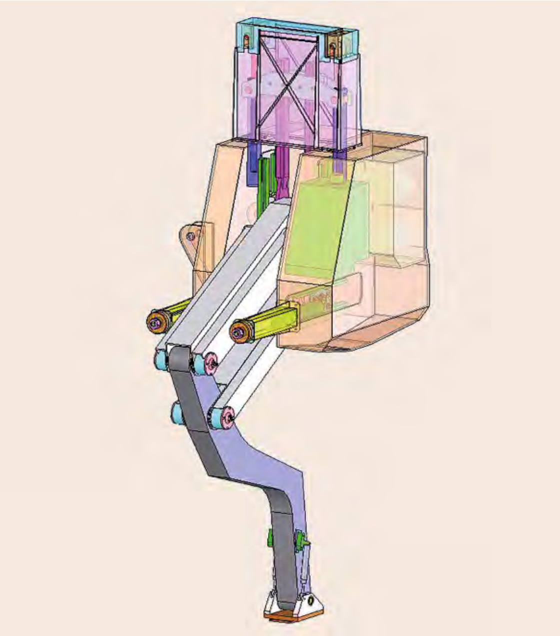

Fig. 4.10 One leg of the ASV walking machine is a parallel robot

Another approach is to specify directly the positions and orientations that are to lie in the workspace and solve the algebraic equations that define the leg constraints to determine the design parameters [4.32, 33]. This is known as kinematic synthesis and yields parallel robots that are asymmetric but have specified reachable and dexterous workspaces, see *McCarthy* and *Soh* [4.34].

4.5.2 Mechanical Advantage

The force amplification properties of a parallel robot are obtained by considering the Jacobians of the individual supporting chains. Let the linear and angular velocity of the platform be defined by the six-vector $\mathbf{v} = (\boldsymbol{v}, \boldsymbol{\omega})^{\mathrm{T}}$, then from the kinematics equations of each of the support legs we have

$$\mathbf{v} = \mathbf{J}_1\dot{\boldsymbol{\rho}}_1 = \mathbf{J}_2\dot{\boldsymbol{\rho}}_2 = \cdots = \mathbf{J}_6\dot{\boldsymbol{\rho}}_6 \;. \tag{4.15}$$

Here we assume that the platform is supported by six chains, but it can be fewer, such as when the fingers of a mechanical hand grasp an object [4.4].

The force on the platform applied by each chain is obtained from the principle of virtual work as

$$\boldsymbol{f}_j = \left(\mathbf{J}_j^{\mathrm{T}}\right)^{-1}\boldsymbol{\tau}_j, \quad j = 1, \ldots, 6 \;. \tag{4.16}$$

There are only six actuated joints in the system so we assemble the associated joint torques into the vector $\boldsymbol{\tau} = (\tau_1, \ldots, \tau_6)^{\mathrm{T}}$. If $\boldsymbol{f}_i$ is the force-torque vector obtained from (4.16) for $\tau_i = 1$ and the remaining torques to zero, then the resultant force-torque $\mathbf{w}$ applied to the platform is

$$\mathbf{w} = (\boldsymbol{f}_1, \boldsymbol{f}_2, \cdots, \boldsymbol{f}_6)\boldsymbol{\tau} \;, \tag{4.17}$$

or

$$\mathbf{w} = \boldsymbol{\Gamma}\boldsymbol{\tau} \;. \tag{4.18}$$

The elements of the coefficient matrix $\boldsymbol{\Gamma}$ define the mechanical advantage for each of the actuated joints. In the case of a Stewart platform the columns of this matrix are the Plücker coordinates of the lines along each leg [4.29].

The principle of virtual work yields the velocity of the platform in terms of the joints rates $\dot{\boldsymbol{\rho}}$ as

$$\boldsymbol{\Gamma}^{\mathrm{T}}\mathbf{v} = \dot{\boldsymbol{\rho}} \;. \tag{4.19}$$

Thus, the inverse of $\mathbf{\Gamma}$ defines the speed ratios between the actuated joints and the end-effector. The same equation can be obtained by computing the derivative of the geometric constraint equations (4.14), and $\mathbf{\Gamma}$ is the *Jacobian* of the parallel robot system [4.35].

The Jacobian $\mathbf{\Gamma}$ is used in parameter optimization algorithms to design parallel robots [4.36] with isotropic mechanical advantage. The square root of the determinant $|\mathbf{\Gamma}\mathbf{\Gamma}^{\mathrm{T}}|$ measures the six-dimensional volume spanned by the column vectors $\boldsymbol{f}_j$. The distribution of the percentage of this volume compared to its maximum within the workspace is also used as a measure of the overall performance [4.37, 38]. A similar performance measure normalizes this Jacobian by the maximum joint torques available and the maximum component of force and torque desired, and then seeks an isotropic design [4.39].

4.5.3 Specialized Parallel Robots

Another approach to the design of parallel robots has been to separate their functionality into orientation and translational platforms. *Tsai* and *Joshi* [4.40] and *Jin* and *Yang* [4.41] survey designs for a class of parallel chains that generate pure translation. *Kong* and *Gosselin* [4.42] and *Hess-Coelho* [4.43] do the same for parallel chains that provide rotational movement in space.

4.6 Mechanical Structure

For the purposes of dynamic modeling, the links of a robot are generally considered to be rigid. However, a robot is not a rigid structure. Like all structures it deflects under applied loads, such as its own weight and the weight of the payload, termed gravity loading; see Figs. 4.11 and 4.12. The issue is a matter of degree. The more force that is needed to cause a deflection in the links, the more the robot moves like a connected set of rigid bodies. Rigid robots have links designed to be stiff so the deflections under load are less than the positioning accuracy required for their range of tasks. This allows the dynamic model and control algorithms to ignore link deflection. Most commercially available robot arms are of this type (*Rivin* [4.44]).

It is possible to improve the positioning accuracy of a rigid robot by augmenting a control algorithm that includes a model of link deflection resulting from gravity loading. It is also possible to use strain sensors to measure loads and deflections. These *semirigid* robots assume small structural deflections that are linearly related to known applied loads.

Flexible robots require that the dynamic model include the deflection of its various links under gravity loading as well as under the forces associated with link acceleration, called inertia loading. The robot control algorithms must control the vibration of the system as well its gross motion. Management of vibration may be required even in rigid robots to reduce cycle time when subjected to high dynamic loading at high speeds or when manipulating large payloads.

4.6.1 Links

For industrial robots a critical concern is the link stiffness in bending and in torsion. To provide this stiffness, robot links are designed either as beams or shell (monocoque) structures. Monocoque structures have lower weight or higher strength-to-weight ratios, but are more costly and generally more difficult to manufacture. Cast, extruded, or machined beam-based links are often more cost effective; *Juvinall* and *Marshek* [4.45], and *Shigley* and *Mischke* [4.46, 47]

Another important consideration is whether the link structure includes bolted, welded, or adhesive bonded assemblies of cast, machined, and fabricated elements. Screw and bolted connections may seem straightforward, inexpensive, and easily maintained, but the inevitable deflection of a link even in the manufacturing process introduces creep in these multiple element assemblies that changes the dimensions and performance of the robot. Welded and cast structures are much less susceptible to creep and the associated hysteresis deformation, though in many cases they require secondary manufacturing operations such as thermal stress relieving and finish machining.

The minimum practical wall or web thickness for castings may be thicker than necessary for stiffness. Thin walls can be achieved with structural skin (mono-

Fig. 4.11 The hydraulic Skywash aircraft cleaning robot

Fig. 4.12 DeLaval Cow Milking System features hydraulic robot with machine vision guided positioning (VIDEO 643)

coque) structures but this is offset by the potential for denting, permanent deformation, and damage in the event of slight collisions. Therefore, both the performance and application requirements must be considered when selecting the construction and fabrication details of the robot.

Performance- and application-specific materials and geometry are used to reduce the weight of the links and therefore the associated gravity and inertial loading. For structures that move in a straight line, aluminum or magnesium alloy extrusions of constant cross section are convenient. Carbon and glass-fiber composites provide lower mass for robots that require high acceleration (painting robots). Thermoplastic materials provide low-cost link structures though at reduced load capacity. Stainless steel is often used in robots for medical and food service applications. The longer links on serial chain robots often are designed to taper in cross section or wall thickness to reduce the associated inertial loading.

4.6.2 Joints

Joints for most robots allow either rotary or linear movement, termed revolute and prismatic joints. Other joints that are available are the ball-in-socket, or spherical joint, and the Hooke-type universal joint.

Integration of the mechanical structure of the robot with its joint mechanism, which includes the actuator and joint motion sensor, is a source of structural flexibility. Precision is reduced when deformation in the joint at its bearings can reduce gear and shaft preloads, allowing undesirable backlash and free play. Structural flexibility can also introduce changes in gear center spacing, introducing forces and torques and associated deflection, binding, jamming, and wear.

4.7 Joint Mechanisms

A robot joint mechanism consists of at least four major components: the joint axis structure, an actuator, transmission, and state sensor (usually for position and velocity feedback, but force sensors are also common).

For low-performance manipulators that accelerate the payload at less than a peak of $0.5\,g$, system inertia is not as important as gravity forces and torques. This means the actuators can be placed near the joints, and their suspended weight compensated by using counterbalancing masses, springs, or gas pressure.

In high-performance robots where peak payload accelerations reach $3-10\,g$ or more, minimizing system inertia is important. The actuators are placed near the first joint axis of a serial link manipulator to minimize its inertial contribution, and drive linkages, belts, cables or spaced gear stages are used to drive the joints.

While a longer transmission distance can reduce mass and gravity moments and inertia, it introduces flexibility and thus reduces the system stiffness. The design of the actuator placement and transmission for each joint is a trade-off between weight, inertia, stiffness, and complexity. This choice dictates the major physical characteristics of a manipulator design. To illustrate this point, consider the Adept 1 assembly robot with four degrees of freedom, each a different structure. The first axis has a direct motor drive. The second axis is driven by a steel band drive, and the third by a synchronous belt drive. Finally, the fourth axis uses a linear ball–screw drive. For a variety of useful joint mechanisms *Sclater* and *Chironis* [4.48].

4.7.1 Joint Axis Structures

Revolute Joints

Revolute or rotary motion joints are designed to perform pure rotation while minimizing other displacements and motions. The most important measure of the quality of a revolute joint is its stiffness or resistance to all undesired motion. Key factors to be considered in design for stiffness are shaft diameter, mounting configuration and preloading of the bearings and proper clearances and tolerances. Shaft diameter and bearing size are not always based on load-carrying capacity; rather, they often will be selected to be compatible with a rigid mounting configuration and also have a bore large enough to pass cables, hoses, and even drive elements for other joints. Because joint shafts will frequently be torque-transmitting members, they and their supporting structure must be designed both for bending and torsional stiffness. The first axis of the PUMA robot is an example of such a joint with its large-diameter tubular configuration.

An important factor in maintaining stiffness in a revolute joint is the choice of bearing-mounting configuration. The mounting arrangement and mount must be designed to accommodate manufacturing tolerances, thermal expansion and bearing preload. Axial preloading of ball or tapered roller bearings improves system accuracy and stiffness by minimizing both axial and radial play. Preloads can be achieved through selective assembly or elastic (spring) elements, shim spacers, threaded collars, four-point contact bearings, duplex bearing arrangements, and tight manufacturing tolerances.

Prismatic Joints

There are two basic types of prismatic or linear motion joints: single-stage and telescoping joints. Often a prismatic joint and its associated link and actuator are combined as a linear actuator. Single-stage joints are made up of a moving surface that slides linearly along a fixed surface. Telescoping joints are essentially sets of nested or stacked single-stage joints. Single-stage joints feature simplicity and high stiffness, whereas the primary advantage of telescoping joints is their retracted-state compactness and large extension ratio. Telescoping joints have a lower effective joint inertia for some configurations and motions because part of the joint may remain stationary or move with reduced acceleration.

The primary functions of bearings in prismatic joints are to facilitate motion in a single direction and to prevent motion in all other directions. Preventing these unwanted motions poses the more challenging design problem. Deformations in the structure can distort the bearing. In severe cases, ball or roller deflection under load may cause binding, which precludes motion. For high-precision prismatic joints, ways must be straight and precise along their entire length which may be several meters. The required precision grinding on multiple surfaces can be costly. Bulky covers may be required to shield and seal a prismatic bearing and way assembly.

The primary criterion for evaluating higher number (in or near the wrist or end-effector) linear motion joints or axes is the stiffness-to-weight ratio. Achieving a good stiffness-to-weight ratio requires the use of a hollow or thin-walled structure rather than solid members for the moving elements.

Bearing spacing is extremely important in design for stiffness. If this spacing is too short, system stiffness will be inadequate no matter how great the bearing stiffness. A major cause for failure in prismatic joints is surface fatigue wear (brinelling) of the ways caused by excessive ball loading due to high preload, moment loads and shock loads.

The large exposed precision surfaces in most prismatic joints make them much more sensitive than revolute joints to contamination, improper handling and environmental effects. They are also significantly more difficult to manufacture, properly assemble, and align.

Common types of sliding elements for prismatic motion are bronze or thermoplastic impregnated bushings. These bushings have the advantage of being low in cost, of having relatively high load capacity, and of working with unhardened or superficially hardened (i. e., plated or anodized) surfaces. Because the local or contact stress on the moving element is distributed and is low this element may be made of thin tube or an extruded shape. Another type of bushing in common use is the ball bushing. Ball bushings have the advantages of lower friction and greater precision than plain bushings. However, they require that the contacting surface of the joint be heat treated or hardened (generally to Rc 55 or greater) and of sufficient case and wall thickness to support the ball point contact loads and resulting high stresses.

Ball and roller slide assemblies are commonly used in robot prismatic joints. There are two basic categories of these slides; recirculating and non-recirculating. Non-recirculating ball and roller slides are used primarily for short-travel applications. They feature high precision and very low friction at the expense of being more sensitive to shock and relatively poor at accommodating moment loading. Recirculating ball slides are somewhat less precise but can carry higher loads than non-recirculating ball slides. They can also be set up to handle relatively large moment loads. Travel range can be up to several meters. Commercial recirculating ball slides and ways have greatly simplified the design and construction of linear axes, particularly in gantry and track mounted manipulators.

Another common type of prismatic robot joint is made up of cam followers, rollers, or wheels rolling on extruded, drawn, machined, or ground surfaces. In high-load applications the surfaces must be hardened before they are finish ground. Cam followers can be purchased

Fig. 4.13 RobotWorld is an integrated workcell with multiple robot modules that move on air bearings

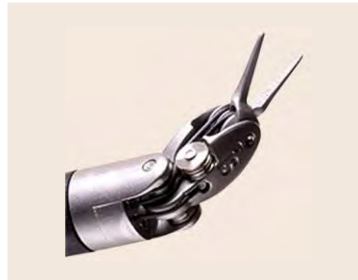

Fig. 4.14 Wrist for surgery has no singularities within range of motion. Features tungsten cable actuation (after [4.49])

with eccentric mounting shafts to facilitate setup and adjustment. Elastomer rollers provide quiet, smooth operation.

Two less common types of linear or prismatic joints feature flexures and air bearings. Flexure-based joints, whose motion results from elastic bending deformations of beam support elements, are used primarily for small, high-resolution, quasilinear motions. Air bearings require smooth surfaces and close control of tolerances as well as a constant supply of filtered, oil-free compressed air. Two- and three-degree-of-freedom air bearings (x, y, θ) can enable multiaxis motion with few moving parts (Fig. 4.13).

Joint Travel

For revolute joint configurations, the shoulder and elbow joints and links determine the gross volume of the work envelope (reachable workspace) of a robot manipulator arm. The wrist joints generally determine the orientation range (dexterous workspace) about a point within this work envelope. Larger joint travel may increase the number of possible manipulator configurations that will reach a particular location (increased task space). Wrist joint travel in excess of 360° and up to 720° can be useful for situations requiring controlled-path (e.g., straight-line) motion, synchronized motion such as small part assembly on a moving conveyor belt, or sensor-modified motions as in using machine vision to select and guide picking jumbled items from a bin. Continuous last-joint rotation is desirable in certain cases like loading or unloading a rotating machine or mating threaded parts.

Additional joints and links, sometimes in the robot but more often in the end-effector, and specialized tooling also serve to increase the task space of a robot. Continuous and controlled-path robot motion requires planning to avoid singularities (regions where two or more joints may become aligned or nearly aligned) and the resulting unstable end-effector motion in these regions. Manipulator design coordinated with a well-planned workcell layout can improve the useful task space by placing critical motions well away from singularity regions. For example, a standard three-axis robot wrist has singularities 180° apart, which can be increased to 360° by implementing a somewhat more complex reduced singularity wrist. Such a wrist is used in a sheep-shearing robot to achieve multiple, long, continuous, smooth, constant-velocity, sensor-guided passes over the contoured body of a sheep to shear its wool [4.50, 51]. Figure 4.14 shows a wrist used for minimally-invasive surgery that has no singularities within its range of motion [4.49].

4.8 Actuators

Actuators supply the motive power for robots. Most robot actuators are commercially available components, which are adapted or modified, as necessary, for a specific robot application. Three commonly used actuator types are electromagnetic, hydraulic and pneumatic.

4.8.1 Electromagnetic Actuators

The most common types of actuators in robots today are electromagnetic actuators.

Electric Servomotors

Most robot manipulators use servomotors as a power source. Servomotors are designed to accurately follow the desired position, velocity and torque which change frequently and sometimes abruptly. They have structures similar to ordinary electric motors, but with low inertia and large torque capably for high accelerations. Typical servomotors used for robotic applications are permanent magnet (PM) DC motors and brushless DC (BLDC) motors.

PM DC motors are widely used as a servomotor because of high torque, speed controllability over a wide range, well-behaved torque-speed characteristics, and adaptability to various types of control methods. The DC motor converts electrical energy into rotational or linear mechanical energy. It comes in many different types and configurations. The lowest-cost PM motors use ceramic (ferrite) magnets and robot toys and hobby robots often use this type of motor. A PM motor with a rare-earth (neodymium-iron-boron), NEO magnet stator produces the most torque and power for its size.

Brushless motors, also called AC servomotors or brushless DC motors, are widely used in industrial robots (Figs. 4.15 and 4.16). They substitute magnetic or optical sensors and electronic switching circuitry for the graphite brushes and copper bar commutator used in brush-type DC motors, thus eliminating the friction, spark-ing, and wear of commutating parts. Brushless motors generally have good performance at low cost because of the decreased complexity of the motor. However, the controllers for these motors are more complex and expensive than brush-type motor controllers. A passive multi-pole neodymium magnet rotor and a wire-wound iron stator of a brushless motor provide good heat dissipation and excellent reliability. Linear brushless motors function like unrolled rotary motors. They typically have a long, heavy, multiple magnet passive stator and a short, lightweight, electronically commutated wire-wound forcer (slider).

Fig. 4.15 The Baldor AC servomotor

Fig. 4.16 The Anorad brushless linear motor

Modeling of DC Motors and BLDC Motors. Both DC and BLDC motors can be described by almost identical equations although they have different structures, *de Silva* [4.52]. Fig. 4.17. The motor torque τ_m generated at the motor is given by,

$$\tau_m = K_t i_a \,, \tag{4.20}$$

where K_t is the torque constant [N m/A] and i_a is the armature current [A].

When the rotor is rotating, the back electromotive force (emf) v_b is induced as follows,

$$v_b = K_b \omega_m \,, \tag{4.21}$$

where K_b is the back emf constant [V/(rad/s)] and ω_m is the angular speed of the motor [rad/s].

The circuit equation is given by

$$v_a = R_a\, i_a + L_a \frac{\mathrm{d}i_a}{\mathrm{d}t} + v_b \,, \tag{4.22}$$

where v_a is the armature voltage (supply voltage to the armature) [V], R_a and L_a are the resistance [Ω] and inductance [H] of the armature winding, respectively.

Lastly, the mechanical equation is described by

$$J\frac{\mathrm{d}\omega_m}{\mathrm{d}t} + B\omega_m = \tau_m - \frac{\tau_l}{r} \,, \tag{4.23}$$

where J is the equivalent moment of inertia referred to the motor shaft [kg m^2], B is the equivalent viscous-friction coefficient referred to the motor shaft [N m/rad/s], τ_l is the load torque [N m], and r is the gear ratio. The quantities J and B are given by

$$J = J_m + \frac{J_l}{r^2}, \quad B = B_m + \frac{B_l}{r^2} \,, \tag{4.24}$$

where J_m and B_m are related to the motor including the gear connected to the motor shaft and J_l and B_l are referred to the load including the gear connected to the load shaft.

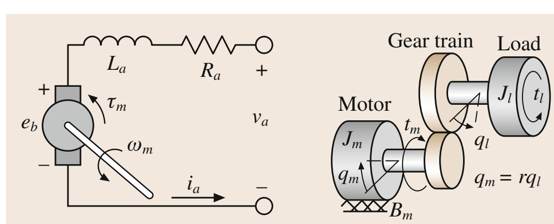

Fig. 4.17 Servomotor models

The four equations above can be represented as the block diagram in Fig. 4.18.

In the servomotors, the electrical time constant $\tau_e = L_a/R_a$ and mechanical time constant $\tau_m = J/B$ have effects on their performance. The electrical time constant is much smaller than mechanical time constant because of the armature inductance is usually negligible. Considering this factor, the angular speed of the motor is described in terms of the armature voltage v_a and load torque τ_l as follows

$$\omega_m(s) = \frac{1}{JR_a\, s + (R_a\, B + K_t K_b)} \left(K_t v_a(s) - R_a \frac{\tau_l(s)}{r} \right) . \quad (4.25)$$

The above equation is frequently used in simulations of both DC motor and BLDC motors.

Stepper Motors. Small, simple robots, such as benchtop adhesive dispensing robots, frequently use stepper or pulse motors of the permanent magnet (PM) hybrid type or sometimes the variable reluctance (VR) type (Fig. 4.19). These robots use open-loop position and velocity control. They are relatively low in cost and interface easily to electronic drive circuits. Microstep control can produce 10 000 or more discrete robot joint positions. In open-loop step mode the motors and robot motions have a significant settling time, which can be damped either mechanically or through the application of control algorithms. Power-to-weight ratios are lower for stepper motors than for other types of electric motors. Stepper motors operated with closed-loop control function similarly to direct-current (DC) or alternating-current (AC) servomotors (Fig. 4.20).

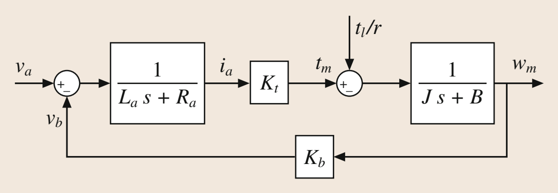

Fig. 4.18 Block diagram for servomotors

Fig. 4.19 The Sony robot uses open-loop permanent-magnet stepper motors

Permanent-Magnet DC Motor. The permanent-magnet, direct-current, brush-commutated motor is widely available and comes in many different types and configurations. The lowest-cost permanent-magnet motors use ceramic (ferrite) magnets. Robot toys and hobby robots often use this type of motor. Neodymium (NEO) magnet motors have the highest energy-product magnets, and in general produce the most torque and power for their size.

Ironless rotor motors, often used in small robots, typically have copper wire conductors molded into epoxy or composite cup or disk rotor structures. The advantages of these motors include low inductance, low friction, and no cogging torque. Disk armature motors have several advantages. They have short overall lengths, and because their rotors have many commutation segments, they produce a smooth output with low torque ripple. A disadvantage of ironless armature motors is that they have a low thermal capacity due to low mass and limited thermal paths to their case. As a result, when driven at high power levels they have rigid duty-cycle limitations or require forced-air cooling.

4.8.2 Hydraulic Actuators

Hydraulic actuators, chosen as power sources for the earliest industrial robots, offer very large force capability and high power-to-weight ratios. They convert hydraulic power into useful mechanical energy. The mechanical motion produced may be linear for hy-

Fig. 4.20 The Adept robot uses closed-loop control and variable-reluctance motors (VIDEO 644)

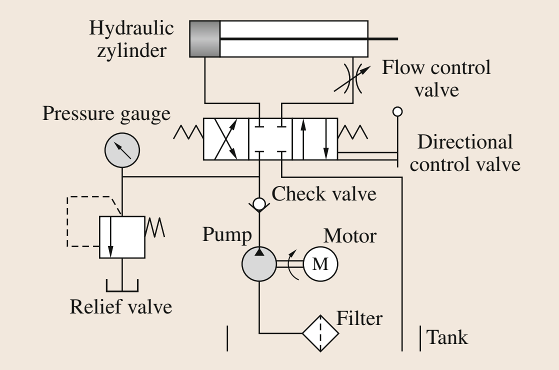

Fig. 4.21 General hydraulic circuit

draulic cylinders or rotary for hydraulic motors and vane actuators.

Figure 4.21 shows the basic hydraulic circuit composed of oil tank, hydraulic pump, check valve, relief valve, directional control valve and hydraulic actuator. Hydraulic fluid pressurized by the hydraulic pump is conveyed to the hydraulic machine to perform the specified task. To this end, the pressure, flow, and direction of hydraulic fluid is changed by the hydraulic control valves such as a pressure control valve, flow control valve, and directional control valve, respectively. The directional control valve changes the flow direction of the hydraulic fluid which is pressurized in the hydraulic pump and thus the direction of actuator motion. The flow control valve changes the flow rate of hydraulic fluid flow and thus the speed of the hydraulic actuator. For safety, the highest pressure is limited by the pressure control valve such as a relief valve.

Hydraulic actuators have several advantages and disadvantages due to the use of high pressure fluid. They can offer very large force or torque and high power-to-weight ratios. Both linear and rotary motions are readily available with small inertia of the moving part. However, the hydraulic power supply is bulky and the cost of the proportional, fast-response servovalves are high. Leaks and maintenance issues have limited the use and applica-tion of hydraulically powered robots.

There have been many applications of hydraulic actuators to robotics. For high forces or torques and speeds, hydraulic servo actuators out-perform current electromagnetic actuators. With proper design, leakage can be virtually eliminated, *Hollerbach* et al. [4.53]. Figure 4.22 shows some typical applications of hydraulic actuators, [4.54–56].

4.8.3 Pneumatic Actuators

Pneumatic actuators are similar to hydraulic actuators. Pneumatic actuators convert energy (in the form of compressed air) into mechanical motion, which may be linear or rotary. Pneumatic actuators are primarily found in simple manipulators. Typically they provide uncontrolled motion between mechanical limit stops. These actuators provide good performance in point-to-point motion. They are simple to control and are low in cost. Pneumatic motors have several advantages over electric motors. They are relatively safe in the explosive environment. They are also less affected by ambient temperature and humidity than electric motors. Although a few small actuators may be run with typical factory air supplies, extensive use of pneumatic-actuated robots requires the purchase and installation of a costly dedicated compressed-air source. Pneumatic actuators have low energy efficiency.

Pneumatic systems consist of pneumatic generator, pneumatic valves, pneumatic actuator and pipes. A pneumatic generator produces compressed air using an air compressor. Pneumatic valves are used to control the pressure, flow rate and direction. The mechanical motion produced may be linear for pneumatic cylinders or rotary for pneumatic motors.

Pneumatic actuators are not used for applications requiring large forces or torques since they produce less power than hydraulic actuators or electric actuators. However, they are used in robot hands or artificial muscles, which require high power-to-weight ratios. Pneumatic artificial muscles are contractile or extensional devices operated by pressurized air filling a pneumatic bladder. They are usually grouped in the agonist

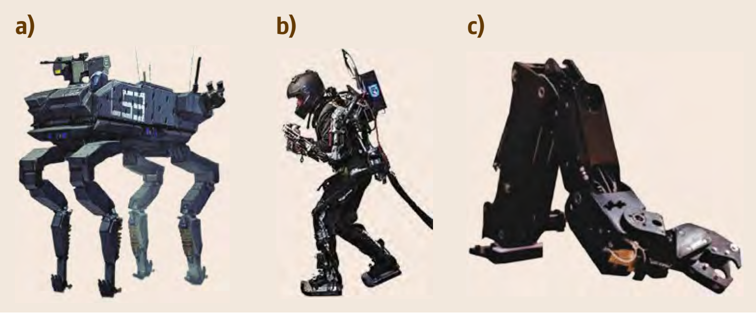

Fig. 4.22a–c Applications of hydraulic actuators to robot: **(a)** BigDog (Boston dynamics) (VIDEO 645), **(b)** Sarcos exosceleton (VIDEO 646) (Raytheon) **(c)** Magnum 7 (International Submarine Engineering)

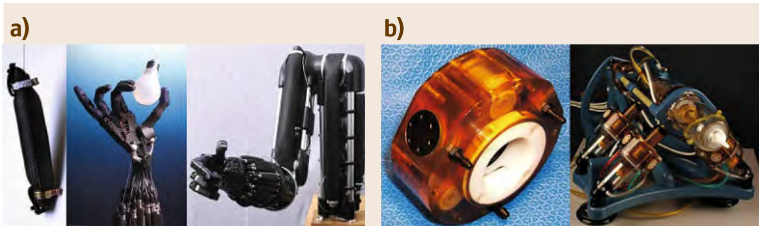

Fig. 4.23a,b Applications of pneumatic actuator: **(a)** robot hand and arm with artificial muscle (Shadow robot) and **(b)** pneumatic step motor and MrBot (Urobotics, Johns Hopkins)

and antagonist pairs. Furthermore, they can be used for medical robots since they are not affected by magnetic field, and for robots in explosive environments because there is no electrical arcing that exists in electromagnetic actuators. Figure 4.23 shows some robotic applications of pneumatic actuators [4.57, 58].

4.8.4 Other Actuators

A wide variety of other types of actuators have been applied to robots. A sampling of these include, thermal, shape-memory alloy (SMA), bimetallic, chemical, piezoelectric, magnetostrictive, electroactive polymer (EAP), bladder, and micro-electromechanical system (MEMS) actuators (see Figs. 4.24 and 4.25). Most of these actuators have been applied to research and special application robots rather than volume production industrial robots. An example of a piezoelectric actuator powered robot is the six-axis PI (Physik Instrumente) piezo hexapod with sub-nanometer resolution shown in Fig. 4.26.

Fig. 4.24 The artificial muscle EAP motor

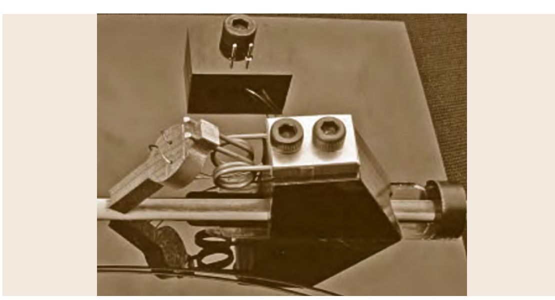

Fig. 4.25 The Elliptec piezoelectric motor

4.8.5 Transmissions

The purpose of a transmission or drive mechanism is to transfer mechanical power from a source to a load. The design and selection of a robot drive mechanism requires consideration of motion, load, and power requirements and the placement of the actuator with respect to the joint. The primary considerations in transmission design are stiffness, efficiency, and cost. Backlash and windup impact drive stiffness especially in robot applications where motion is constantly reversing and loading is highly variable. High transmission stiffness and low or no backlash result in increased friction losses. Most robot transmission elements have good efficiencies when they are operating at or near their rated power levels but not necessarily when lightly loaded. Larger than necessary drives add weight, inertia and friction loss to the system. Underdesigned drives have lower stiffness, can wear rapidly in continuous or in high duty cycle operation or fail due to accidental overloads.

Joint actuation in robots is generally performed by drive mechanisms which interface the actuator (mechanical work source) to the robot links through the joints in an energy-efficient manner. A variety of drive mechanisms are incorporated in practical robots. The transmission ratio of the drive mechanism sets the torque, speed, and inertia relationship of the actuator to the link. Proper placement, sizing, and design of the drive mechanisms set the stiffness, mass, and overall operational performance of the robot. Most modern robots incorporate efficient, overload damage resistant, back-driveable drives.

Fig. 4.26 A six-axis Physik Instrumente (PI) piezo hexapod with sub-nanometer resolution (VIDEO 648)

Direct Drives

The direct drive is kinematically the simplest drive mechanism. In the case of pneumatic or hydraulic actuated robots, the actuator is directly connected between the links. Electric direct-drive robots employ high-torque, low-speed rotary or linear motors directly interfaced to the links. The complete elimination of free play and smooth torque transmission are features of a direct drive. However, there is often a poor dynamic (inertia ratio) match of the actuator to the link requiring a larger, less energy efficient, actuator.

Band Drives

A variant of direct drive is band drive. A thin alloy steel or titanium band is fixed between the actuator shaft and the driven link to produce limited rotary or linear motion. Drive ratios in the order of up to 10 : 1 (10 actuator revolutions for 1 revolution of the joint) can be obtained. Actuator mass is also moved away from the joint – usually toward the base, to reduce robot inertia and gravity loading. It is a smoother and generally stiffer drive than a cable or belt drive.

Belt Drives

Synchronous (toothed) belts are often employed in drive mechanisms of smaller robots and some axes of larger robots. These function much the same as band drives, but have the ability to drive continuously. Multiple stages (two or three) are occasionally used to produce large drive ratios (up to 100 : 1). Belt tension is controlled with idlers or center adjustment. The elasticity and mass of long belts can cause drive instability and thus increased robot settling time.

Gear Drives

Spur or helical gear drives provide reliable, sealed, low-maintenance power transmission in robots. They are used in robot wrists where multiple axes intersect and compact drive arrangements are required. Large-diameter gears are used in the base joints of larger robots to handle high torques with high stiffness. Gears are often used in stages and often with long drive shafts, enabling large physical separation between actuator and driven joint. For example, the actuator and one stage of reduction may be located near the elbow driving another stage of gearing or differential in a wrist through a long hollow drive shaft (Fig. 4.1).

Planetary gear drives are often integrated into compact gearmotors (Fig. 4.27). Minimizing backlash (free play) in a joint gear drive requires careful design, high-precision and rigid support to produce a drive mechanism which does not sacrifice stiffness, efficiency and accuracy for low backlash. Backlash in robots is controlled by a number of methods including selective assembly, gear center adjustment, and proprietary anti-backlash designs.

Worm Gear Drives

Worm gear drives are occasionally used in low-speed robot manipulator applications. They feature right-angle and offset drive capability, high ratios, simplicity, good stiffness and load capacity. They have poor efficiency, which makes them non-back-driveable at high ratios. This causes the joints to hold their position when unpowered but also makes them prone to damage by attempts to manually reposition the robot.

Proprietary Drives

Proprietary drives are widely used in standard industrial manipulators. The harmonic drive and the rotary vector (RV) drive are two examples of compact, low-backlash, high-torque-capability drives using special gears, cams, and bearings (Figs. 4.28 and 4.29).

Harmonic drives are frequently used in very small to medium-sized robots. These drives have low backlash, but its flexspline allows elastic windup and low stiffness during small reversing movements. RV drives are

Fig. 4.27 The Space Shuttle robot arm has planetary gear joint drives

Fig. 4.28 The harmonic drive (VIDEO 649)

usually used in larger robots, especially those subject to overloads and shock loading.

Linear Drives

Direct-drive linear actuators incorporate a linear motor with a linkage to a linear axis. This linkage is often merely a rigid or flexure connection between the actuator forcer and the robot link. Alternatively, a packaged linear motor with its own guideways is mechanically connected directly to a linear axis. Direct linear electromagnetic drives feature zero backlash, high stiffness, high speeds, and excellent performance but are heavy, have poor energy efficiency, and cost more than other types of linear drives.

Ball Screws

Ball–screw-based linear drives efficiently and smoothly convert rotary actuator motion into linear motion. Typically, a recirculating ball nut mates with a ground and hardened alloy steel screw to convert rotary motion into linear motion. Ball screws can be easily integrated into linear axes. Compact actuator/drive packages are available, as well as components for custom integration. Stiffness is good for short and medium travel, however it is lower for long motions because the screw can only be supported at its ends. Low or zero backlash can be obtained with precision-ground screws. Speeds are limited by screw dynamic stability so rotating nuts enable higher speeds. Low-cost robots may employ plain screw drives featuring thermoplastic nuts on smooth rolled thread screws.

Rack-and-Pinion Drives

These traditional components are useful for long motions where the guideways are straight or even curved. Stiffness is determined by the gear/rack interface and independent of length of travel. Backlash can be diffi-

Fig. 4.29 The Nabtesco RV drive

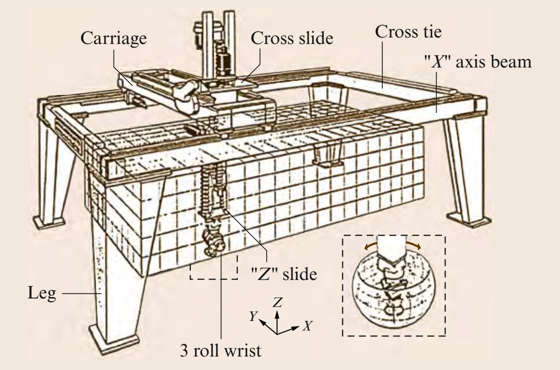

Fig. 4.30 The NASA gantry robot

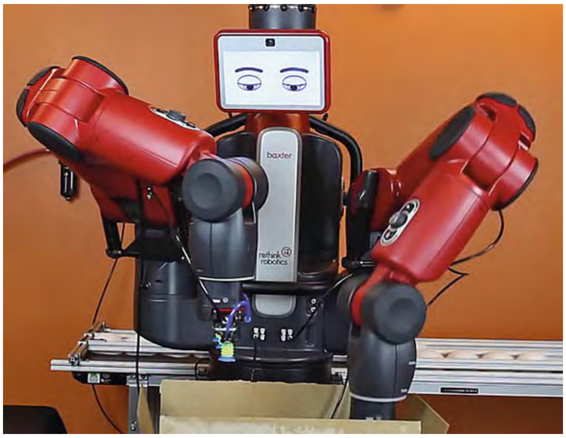

Fig. 4.31 Two-arm collaborative robot with Series Elastic Actuators (after [4.59])

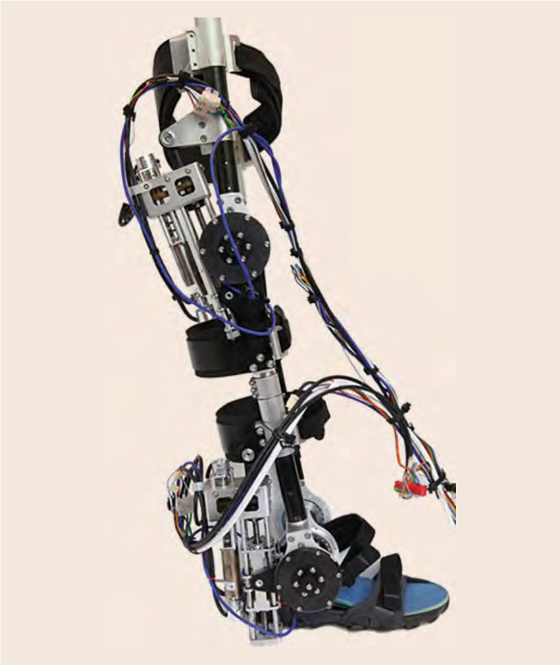

Fig. 4.32 Series Elastic Actuator assembly in knee-ankle-foot gait rehabilitation robot (after [4.60])

cult to control as rack-to-pinion center tolerances must be held over the entire length of travel. Dual pinion drives are sometimes employed to deal with backlash by providing active preload. Forces are generally lower than with screws due to lower ratios. Small-diameter (low teeth count) pinions have poor contact ratios, resulting in vibration. Sliding involute tooth contact requires lubrication to minimize wear. These catalog stock drive components are often used on large gantry robots and track-mounted manipulators (Fig. 4.30).

Compliant Actuators. Compliance in the form of elasticity in a drive can be an asset or a defect in a robot. High overall robot stiffness traditionally produces fast response, high positioning accuracy and simplified control. However the contact and interaction forces developed due to unexpected errors in dealing with the workpieces, tools, workplace and the environment can cause damage to the robot, the surroundings, and injury to persons. By adding controlled and measureable compliance to actuators, the elasticity of the robot can be usefully increased.

One class of reduced stiffness actuator is the Series Elastic Actuator (SEA). It features an elastic output element (spring) with a displacement sensor (measures spring stretch) in series with a stiff actuator and transmission component. With an appropriate controller, the stiff classical position control actuator acts as a force actuator ($F = -kx$), effectively isolating the drive inertia from the load inertia. This limits the forces resulting from collisions or forced compliance often encountered when working in unstructured environments and around persons. SEAs and similar compliant actuators and compliant actuator configurations are discussed in Chap. 69. Collaborative robots are designed to safely work next to or in contact with persons, Fig. 4.31 [4.59], and are an example of robots featuring compliant actuators. Figure 4.32 shows compliant actuators used in an exoskeleton for gait rehabilitation [4.60].

Other Drive Components

Splined shafts, kinematic linkages (four-bar, slider-crank mechanisms, etc.) chains, cables, flex couplings, clutches, brakes, and limit stops are some examples of other mechanical components used in robot drive mechanisms (Fig. 4.8). The Yaskawa RobotWorld assembly and process automation robot system features a magnetically suspended direct electromagnetic drive planar (2 axis) motor with no internal moving parts floating on a virtually frictionless planar air bearing. (Fig. 4.12).

4.9 Robot Performance

Industrial robot performance is often specified in terms of functional operations and cycle time. For assembly robots the specification is often the number of typical pick-and-place cycles per minute. Arc-welding robots are specified with a slow weld pattern and weave speed as well as by a fast repositioning speed. For painting robots, the deposition or coverage rate and spray pattern speed are important. Peak robot velocity and acceleration catalog data are generally just calculated numbers and will vary due to dynamic (inertia) and static (gravity) coupling between robot joints due to configuration changes as a robot moves.

4.9.1 Robot Speed

Maximum joint velocity (angular or linear) is not an independent value. For longer motions it is often limited by servomotor bus voltage or maximum allowable motor speed. For manipulators with high accelerations, even short point-to-point motions may be velocity limited. For low-acceleration robots, only gross motions will be velocity limited. Typical peak end-effector speeds can range up to $20\,\mathrm{m/s}$ for large or fast manipulators.

4.9.2 Robot Acceleration

In most modern manipulators, because the payload mass is small when compared with the manipulator mass, more power is spent accelerating the manipulator than the load. Acceleration affects gross motion time as well as cycle time (gross motion time plus settling time). Manipulators capable of greater acceleration tend to be stiffer manipulators. In high-performance robot manipulators, acceleration and settling time are more important design parameters than velocity or load capacity. Maximum acceleration for some assembly and material handling robots is in excess of $10\,g$ with light payloads.

4.9.3 Repeatability

This specification represents the ability of the manipulator to return repeatedly to the same location. Depending on the method of teaching or programming the manipulator, most manufacturers intend this figure to indicate the radius of a sphere enclosing the set of locations to which the arm returns when sent from the same origin by the same program with the same load and setup conditions. This sphere may not include the target point because calculation round-off errors, simplified calibration, precision limitations, and differences during the teaching and execution modes can cause significantly larger errors than those just due to friction, unresolved joint and drive backlash, servo system gain, and structural and mechanical assembly clearances and play. The designer must seriously consider the real meaning of the required repeatability specification. Repeatability is important when performing repetitive tasks such as blind assembly or machine loading. Typical repeatability specifications range from 1–2 mm for large spot-welding robots to 0.005 mm (5 μm) for precise micropositioning manipulators.

4.9.4 Resolution

This specification represents the smallest incremental motion that can be produced by the manipulator. Resolution is important in sensor-controlled robot motion and in fine positioning. Although most manufacturers calculate system resolution from the resolution of the joint position encoders, or from servomotor and drive step size, this calculation is misleading because system friction, windup, backlash, and kinematic configuration affect the system resolution. Typical encoder or resolver resolution is 10^{14}–10^{25} counts for full-axis or joint travel, but actual physical resolution may be in the range 0.001–0.5 mm. The useful resolution of a multi-joint serial-link manipulator is worse than that of its individual joints.

4.9.5 Accuracy

This specification covers the ability of a robot to position its end-effector at a preprogrammed location in space. Robot accuracy is important in the performance of nonrepetitive types of tasks programmed from a database, or for taught tasks that have been remapped or offset owing to measured changes in the installation.

Accuracy is a function of the precision of the arm kinematic model (joint type, link lengths, angles between joints, any accounting for link or joint deflections under load, etc.), the precision of the world, tool, and fixture models, and the completeness and accuracy of the arm solution routine. Although most higher-level robot programming languages support arm solutions, these solutions usually model only simplified rigid-body kinematic configurations. Thus, manipulator accuracy becomes a matter of matching the robot geometry to the robot solution in use by precisely measuring and calibrating link lengths, joint angles, and mounting positions.

Typical accuracies for industrial manipulators range from ±10 mm for uncalibrated manipulators that have poor computer models to ±0.01 mm for machine-tool-like manipulators that have controllers with accurate kinematic models and solutions and precisely manufactured and measured kinematic elements.

4.9.6 Component Life and Duty Cycle

The three subassemblies in an electrically powered robot with the greatest failure problems are the actuators (servomotors), transmissions, and power and signal cables. Mean time between failures (MTBF) should be a minimum of 5000 h on line, and ideally at least 10 000 operating hours should pass between major component preventive maintenance replacement schedules.

Worst-case motion cycles must be assumed as most current robot installations are used in generally repetitive tasks. Small-motion design-cycle life (less than 5% of joint travel range) for assembly robots should be 20–100 million full bidirectional cycles. Large-motion cycle life (greater than 50% of full joint range) should typically be 5–40 million cycles.

Short-term peak performance is frequently limited by maximum drive loading, whereas long-term, continuous, performance is limited by motor heating. Rather than design for equal levels of short- and long-term performance, cost savings and performance improvements can result from designing for an anticipated duty cycle. This allows the use of smaller, lower-inertia, lighter motors. Industrial robots usually become obsolete and are replaced before they reach their design cycle life.

4.9.7 Collisions

In the course of operation, unforeseen or unexpected situations may occasionally result in a collision involving the manipulator, its tools, the workpiece, or other objects in the workplace. These accidents may result in no, little, or extensive damage, depending in large part on the design of the manipulator. Crash-resistant design options should be considered early in the design process if the time lost or cost of such accidents could be significant. Typical damage due to accidents include fracture or shear failures of gear teeth or shafts, dented or bent link structures, slipping of gears or pulleys on shafts, cut or severely abraded or deformed wires, cables or hoses, and broken connectors, fittings, limit stops or switches. Compliant elements such as overload (slip) clutches, elastic members, and padded surfaces can be incorporated to reduce shock loads and help decouple or isolate the actuators and drive components in the event of such collisions.

4.10 Conclusions and Further Reading

The mechanical design of a robot is an iterative process involving engineering, technical, and application-specific considerations evaluations, and choices. The final design should reflect consideration of detailed task requirements rather than simply broad specifications. Proper identification and understanding of these requirements is a key to achieving the design goals.

Design and choice of specific components involves tradeoffs. A purely static, rigid-body approach to manipulator design is often used, but is not always sufficient. Mechanical system stiffness, natural frequencies, control system compatibility, and intended robot applications and installation requirements must be considered.

There are many opportunities for further reading on the design of the mechanisms and actuation that form the core of a robotic system. A well-known and useful reference for robot design is *Rivin* [4.44].

Craig [4.6] and *Tsai* [4.9] provide the mathematical relations between the mechanical structure of a robot and its workspace and mechanical advantage. *Sclater* and *Chironis* [4.48] is a reprint of a valuable compendium of devices useful for a variety of applications, such as joint drives and transmissions. See *McCarthy* and *Soh* [4.34] for geometric techniques to design specialized mechanisms.

Juvinall and *Marshek* [4.45] and *Shigley* and *Mischke* [4.46, 47] are important references for the design of the components such as the link structure, bearings, and transmissions that are central to the effective mechanical performance of robotic systems.

Although many design decisions can be made through the application of straightforward algorithms and equations, a multitude of other important considerations transform the challenge of robot design into one requiring good engineering judgment.

Video-References

VIDEO 640 A parallel robot
available from http://handbookofrobotics.org/view-chapter/04/videodetails/640
VIDEO 642 Three-fingered robot hand
available from http://handbookofrobotics.org/view-chapter/04/videodetails/642
VIDEO 643 Robotics milking system
available from http://handbookofrobotics.org/view-chapter/04/videodetails/643
VIDEO 644 SCARA robots
available from http://handbookofrobotics.org/view-chapter/04/videodetails/644
VIDEO 645 Big Dog –Applications of hydraulic actuators
available from http://handbookofrobotics.org/view-chapter/04/videodetails/645
VIDEO 646 Raytheon Sarcos exoskeleton
available from http://handbookofrobotics.org/view-chapter/04/videodetails/646
VIDEO 648 PI piezo hexapod
available from http://handbookofrobotics.org/view-chapter/04/videodetails/648
VIDEO 649 Harmonic drive
available from http://handbookofrobotics.org/view-chapter/04/videodetails/649

References

4.1 D.T. Greenwood: *Classical Dynamics* (Prentice Hall, Upper Saddle River 1977)
4.2 F.C. Moon: *Applied Dynamics* (Wiley, New York 1998)
4.3 S.-M. Song, K.J. Waldron: *Machines that Walk: The Adaptive Suspension Vehicle* (MIT Press, Cambridge 1988)
4.4 M.T. Mason, J.K. Salisbury: *Robot Hands and the Mechanics of Manipulation* (MIT Press, Cambridge 1985)
4.5 R.P. Paul: *Robot Manipulators: Mathematics, Programming, and Control* (MIT Press, Cambridge 1981)
4.6 J.J. Craig: *Introduction to Robotics: Mechanics and Control* (Addison-Wesley, Reading 1989)
4.7 O. Bottema, B. Roth: *Theoretical Kinematics* (North-Holland, Amsterdam 1979)
4.8 J.M. McCarthy: *An Introduction to Theoretical Kinematics* (MIT Press, Cambridge 2013)
4.9 L.W. Tsai: *Robot Analysis. The Mechanics of Serial and Parallel Manipulators* (Wiley, New York 1999)
4.10 T. Lozano-Perez: Spatial Planning: A configuration space approach, IEEE Trans. Comput. **32**(2), 108–120 (1983)
4.11 J.C. Latombe: *Robot Motion Planning* (Kluwer, Boston 1991)
4.12 R. Vijaykumar, K. Waldron, M.J. Tsai: Geometric optimization of manipulator structures for working vol-

ume and dexterity. In: *Kinematics of Robot Manipulators*, ed. by J.M. McCarthy (MIT Press, Cambridge 1987) pp. 99–111
4.13 K. Gupta: On the nature of robot workspace. In: *Kinematics of Robot Manipulators*, ed. by J.M. McCarthy (MIT Press, Cambridge 1987) pp. 120–129
4.14 I. Chen, J. Burdick: Determining task optimal modular robot assembly configurations, Proc. IEEE Robotics Autom. Conf. (1995) pp. 132–137
4.15 P. Chedmail, E. Ramstei: Robot mechanisms synthesis and genetic algorithms, Proc. IEEE Robotics Autom. Conf. (1996) pp. 3466–3471
4.16 P. Chedmail: Optimization of multi-DOF mechanisms. In: *Computational Methods in Mechanical Systems*, ed. by J. Angeles, E. Zakhariev (Springer, Berlin, Heidlberg 1998) pp. 97–129
4.17 C. Leger, J. Bares: Automated Synthesis and Optimization of Robot Configurations, Proc. ASME Design Tech. Conf., Atlanta (1998), paper no. DETC98/Mech-5945 CD-ROM
4.18 F.C. Park: Distance metrics on the rigid body motions with applications to mechanism design, ASME J. Mech. Des. **117**(1), 48–54 (1995)
4.19 J.M.R. Martinez, J. Duffy: On the metrics of rigid body displacements for infinite and finite bodies, ASME J. Mech. Des. **117**(1), 41–47 (1995)
4.20 M. Zefran, V. Kumar, C. Croke: Choice of Riemannian metrics for rigid body kinematics, Proc. ASME Design Tech. Conf., Irvine (1996), paper no. DETC96/Mech-1148
4.21 Q. Lin, J.W. Burdick: On well-defined kinematic metric functions, Proc. Int. Conf. Robotics Autom., San Francisco (2000) pp. 170–177
4.22 C. Gosseli: On the design of efficient parallel mechanisms. In: *Computational Methods in Mechanical Systems*, ed. by J. Angeles, E. Zakhariev (Springer, Berlin, Heidelberg 1998) pp. 68–96
4.23 J.V. Albro, G.A. Sohl, J.E. Bobrow, F. Park: On the computation of optimal high-dives, Proc. Int. Conf. Robotics Autom., San Francisco (2000) pp. 3959–3964
4.24 G.E. Shilov: *An Introduction to the Theory of Linear Spaces* (Dover, New York 1974)
4.25 J.K. Salisbury, J.J. Craig: Articulated hands: Force control and kinematic issues, Int. J. Robotics Res. **1**(1), 4–17 (1982)
4.26 J. Angeles, C.S. Lopez-Cajun: Kinematic isotropy and the conditioning index of serial manipulators, Int. J. Robotics Res. **11**(6), 560–571 (1992)
4.27 J. Angeles, D. Chabla: On isotropic sets of points in the plane. Application to the design of robot architectures. In: *Advances in Robot Kinematics*, ed. by J. Lenarčič, M.M. Stanišić (Kluwer, Boston 2000) pp. 73–82
4.28 E.F. Fichter: A Stewart platform-based manipulator: General theory and practical construction. In: *Kinematics of Robot Manipulators*, ed. by J.M. McCarthy (MIT Press, Cambridge 1987) pp. 165–190
4.29 J.P. Merlet: *Parallel Robots* (Kluwer, Boston 1999)
4.30 J.M. Hervé: Analyse structurelle des méchanismes par groupe des déplacements, Mech. Mach. Theory **13**(4), 437–450 (1978)
4.31 J.M. Hervé: The Lie group of rigid body displacements, a fundamental tool for mechanism design, Mech. Mach. Theory **34**, 719–730 (1999)
4.32 A.P. Murray, F. Pierrot, P. Dauchez, J.M. McCarthy: A planar quaternion approach to the kinematic synthesis of a parallel manipulator, Robotica **15**(4), 361–365 (1997)
4.33 A. Murray, M. Hanchak: Kinematic synthesis of planar platforms with RPR, PRR, and RRR chains. In: *Advances in Robot Kinematics*, ed. by J. Lenarčič, M.M. Stanišić (Kluwer, Boston 2000) pp. 119–126
4.34 J.M. McCarthy, G.S. Soh: *Geometric Design of Linkages*, 2nd edn. (Springer, Berlin, Heidelberg 2010)
4.35 V. Kumar: Instantaneous kinematics of parallel-chain robotic mechanisms, J. Mech. Des. **114**(3), 349–358 (1992)
4.36 C. Gosselin, J. Angeles: The optimum kinematic design of a planar three-degree-of-freedom parallel manipulator, ASME J. Mech. Transmiss. Autom. Des. **110**(3), 35–41 (1988)
4.37 J. Lee, J. Duffy, M. Keler: The optimum quality index for the stability of in-parallel planar platform devices, Proc. ASME Design Eng. Tech. Conf., Irvine (1996), paper no. 96-DETC/MECH-1135
4.38 J. Lee, J. Duffy, K. Hunt: A practical quality index based on the octahedral manipulator, Int. J. Robotics Res. **17**(10), 1081–1090 (1998)
4.39 S.E. Salcudean, L. Stocco: Isotropy and actuator optimization in haptic interface design, Proc. Int. Conf. Robotics Autom., San Francisco (2000) pp. 763–769
4.40 L.-W. Tsai, S. Joshi: Kinematics and optimization of a spatial 3-UPU parallel manipulator, J. Mech. Des. **122**, 439–446 (2000)
4.41 Q. Jin, T.-L. Yang: Theory for topology synthesis of parallel manipulators and its application to three-dimension-translation parallel manipulators, J. Mech. Des. **126**(3), 625–639 (2004)
4.42 X. Kong, C.M. Gosselin: Type synthesis of three-degree-of-freedom spherical parallel manipulators, Int. J. Robotics Res. **23**, 237–245 (2004)
4.43 T.A. Hess-Coelho: Topological synthesis of a parallel wrist mechanism, J. Mech. Des. **128**(1), 230–235 (2006)
4.44 E.I. Rivin: *Mechanical Design of Robots* (McGraw-Hill, New York 1988) p. 368
4.45 R.C. Juvinall, K.M. Marshek: *Fundamentals of Machine Component Design*, 4th edn. (Wiley, New York 2005) p. 832
4.46 J.E. Shigley, C.R. Mischke: *Mechanical Engineering Design*, 7th edn. (McGraw-Hill, New York 2004) p. 1056
4.47 J.E. Shigley, C.R. Mischke: *Standard Handbook of Machine Design*, 2nd edn. (McGraw-Hill, New York 1996) p. 1700
4.48 N. Sclater, N. Chironis: *Mechanisms and Mechanical Devices Sourcebook*, 4th edn. (McGraw Hill, New York 2007) p. 512
4.49 Intuitive Surgical EndoWrist Insturments, http://www.intuitivesurgical.com/products/instruments/
4.50 J.P. Trevelyan: Sensing and control for shearing robots, IEEE Trans. Robotics Autom. **5**(6), 716–727 (1989)

4.51 J.P. Trevelyan, P.D. Kovesi, M. Ong, D. Elford: ET: A wrist mechanism without singular positions, Int. J. Robotics Res. **4**(4), 71–85 (1986)

4.52 C. de Silva: *Sensors and Actuators: Control Systems Instrumentation* (CRC, Boca Raton 2007)

4.53 J. Hollerbach, I. Hunter, J. Ballantyne: A comparative analysis of actuator technologies for robotics, Robotics Rev. **2**, 299–342 (1992)

4.54 Boston Dynamics, Waltham, MA, USA: Big Dog Robot, http://www.bostondynamics.com/robot_bigdog.html

4.55 Raytheon, Waltham MA, USA: Sarcos Exoskeleton, http://www.popsci.com/category/tags/raytheon-sarcos-xos

4.56 International Submarine Engineering, Port Coquitlam, BC, Canada: Magnum 7, http://www.ise.bc.ca/manips.html

4.57 Shadow Robot Company, London, UK: Air muscles and pneumatic hands, http://www.shadowrobot.com/tag/muscle-hand

4.58 Johns Hopkins, Baltimore, USA: Pneumatic Stepper Motor and MrBot, http://urobotics.urology.jhu.edu/projects/PneuStep

4.59 The Baxter Robot Rethink Robotics, http://www.rethinkrobotics.com/products/baxter/

4.60 Singapore Institute for Neurotechnology, NeuroRehabilitation Laboratory: http://www.sinapseinstitute.org/projects/neurorehabilitation